The wheat 55K SNP-based exploration of loci for spikelet number per spike from a tetraploid wheat (*Triticum turgidum* L.) recombinant inbred line population derived from a Chinese landrace 'Ailanmai' and a wild emmer accession

Ziqiang Mo[1, #], Jing Zhu[1, #], Jiatai Wei[1], Jieguang Zhou[1], Qiang Xu[1], Huaping Tang[1], Yang Mu[1], Qiantao Jiang[1], Yaxi Liu[1], Guoyue Chen[1], Jirui Wang[1], Pengfei Qi[1], Zhien Pu[2], Guangdeng Chen[3], Yuming Wei[1], Youliang Zheng[1], Xiujin Lan[1, *], Jian Ma[1, *]

[1]*State Key Laboratory of Crop Gene Exploration and Utilization in Southwest China, Triticeae Research Institute, Sichuan Agricultural University, Chengdu, 611130, China*

[2]*College of Agronomy, Sichuan Agricultural University, Chengdu, 611130, China*

[3]*College of Resources, Sichuan Agricultural University, Chengdu, 611130, China*

# contributed equally to this paper.

*Authors for correspondence:

Dr. Jian Ma, E-mail: jianma@sicau.edu.cn

Dr. Xiujin Lan, E-mail:lanxiujin@163.com

Tel: +86 28 86293115; Fax: +86 28 82650350

Key message

The wheat 55K SNP array was firstly and successfully applied to construct a genetic map and explore two major and novel QTL for SNS in a tetraploid wheat RIL population.

Abstract

Spikelet number per spike (SNS) is a key factor in determining kernel number per spike which has a great effect on wheat grain yield. Modern wheat breeding narrows genetic diversity among cultivars leading to a detrimental effect on future wheat improvement. It is thus of great significance to explore new genetic resources for SNS to increase wheat yield. Here, a tetraploid landrace 'Ailanmai' × wild emmer wheat recombinant inbred line (RIL) population was used to construct a high-density genetic map using the wheat 55K single nucleotide polymorphism (SNP) array. Our results showed that the genetic and physical locations of 94.83% (6204) of the mapped markers were consistent. Subsequently, fourteen quantitative trait loci (QTL) for SNS explaining 4.23-27.26% of the phenotypic variation were identified. *QSns.sau-AM-2B.3* and *QSns.sau-AM-3B.2* were considered as major and novel QTL and their combination had the largest effect and increased SNS by 17.47%. In the physical intervals of *QSns.sau-AM-2B.3* and *QSns.sau-AM-3B.2*, some development-related genes were predicted to participate in the spikelet growth and affect SNS. Additionally, significant correlations between SNS and other agronomic traits like significant and positive correlation between SNS and thousand kernel weight were detected and analyzed. Our findings demonstrated the feasibility of wheat 55K SNP array in genetic mapping of tetraploid wheat and provided an example of exploring outstanding genetic resources from wheat related species for further utilization in common wheat improvement.

Introduction

Wheat (*Triticum* sp.) is one of the most widely planted crops globally and provides about 20% of the calories consumed by mankind (http://www.fao.org/faostat). With the development of modern society, breeding high-yield wheat cultivars is considered as a sustainable approach to meet the demands of a growing human population.

As we know, the wheat grain yield is composed of spike number per unit area (SNPA), kernel number per spike (KNS), and kernel weight (KW). Additionally, KNS is jointly determined by spikelet number per spike (SNS) and kernel number per spikelet. SNS depends on the number of lateral spikelets produced before the spike meristem transitions to the terminal spikelet which is a complex quantitative trait greatly affected by genetic and environmental factors (Gao et al. 2019; Kuzay et al. 2019). Hence, researching the genetic mechanism of SNS at the QTL level will give us more insight into the role of SNS in yield formation (Wang et al. 2018; Ma et al. 2019a; Yao et al. 2019; Chen et al. 2020).

So far, a few genes are reportedly related to spikelet number and morphology in wheat. For example, the *WHEAT FRIZZY PANICLE* (*WFZP*) gene encodes a member of the APETALA2/ethylene response transcription factor (AP2/ERF) family, which influences the supernumerary spikelet trait in common wheat (Dobrovolskaya et al. 2015). Regulatory expression of the two pivotal flowering genes, *Photoperiod-1* (*Ppd-1*) and *FLOWERING LOCUS T* (*FT*), can increase the number of fertile spikelets (Boden et al. 2015). The inflorescence growth rate and the development of paired spikelets are controlled by the *TEOSINTE BRANCHED1* (*TB1*) expression level (Dixon et al. 2018). *WHEAT ORTHOLOG OF APO1* (*WAPO1*) is the ortholog of the rice *APO1* and affect spikelet number in wheat (Kuzay et al. 2019). Overexpression of *TaTFL-2D* increases the number of wheat spikelet and floret (Wang et al. 2017). The wheat transcription factor gene *TaNAC67* participates in the regulation of spike length and spikelet number (Zhang et al. 2019).

Given its important role in yield formation, more loci for SNS should be identified and utilized. However, modern wheat breeding reduces the genetic diversity among cultivars and narrows the genetic basis of common wheat leading to a detrimental effect on future wheat improvement (Tanksley and McCouch 1997; Cavanagh et al. 2013; Sthapit et al. 2020). Fortunately, a great quantity of undeveloped genetic resources from wheat related species may effectively meet the challenges of future wheat production (Reynolds et al. 2011; Longin and Reif 2014; Martínez-Moreno et al. 2020).

As the progenitor of modern cultivated tetraploid and hexaploid wheat, wild emmer wheat (*T. turgidum* subsp. *dicoccoides*) is the secondary gene source of common wheat. It possesses rich genetic diversity in resistance to various diseases, important agronomic traits and outstanding environmental adaptabilities, and plays a significant role in wheat breeding (Tanksley and McCouch 1997; Xie and Nevo 2008; Yu et al. 2020). For example, *Yr15* derived from wild emmer wheat results in resistance to yellow rust (Klymiuk et al. 2018). And the reduced-function allele *GNI-A1* increases the number of fertile florets per spikelet (Sakuma et al. 2019). Hence, exploiting the genetic resources of wild emmer wheat is extremely crucial to solve the bottlenecks encountered in current wheat breeding. Wheat landraces are also important basic materials for wheat improvement and breeding (Lin et al. 2020). They are precious crop resources preserved under long-term natural selection and human intervention, with strong adaptability to local environmental conditions and corresponding production potential (Lopes et al. 2015; Crossa et al. 2016), harboring some peculiar gene resources yet to be exploited for wheat improvement.

In the current research, we constructed a high-quality genetic map in a tetraploid wheat population developed from the cross between a Chinese wheat landrace ‘Ailanmai’ and a wild emmer wheat accession using the wheat 55K SNP array. Further, we identified QTL for SNS based on phenptypes measured from multiple environments and the constructed genetic map. Candidate genes in the intervals of the

wild emmer genome (Avni et al. 2017) harboring major and stably expressed SNS QTL were predicted. The correlations between SNS and other agronomic traits including plant height (PH), anthesis date (AD), productive tiller number (PTN), spike length (SL), spike extension length (SEL), kernel number per spike (KNS), and thousand kernel weight (TKW) were also detected and analyzed. Current results broaden our understanding of the application potential of wheat related species in common wheat improvement.

Materials and methods

Plant materials

A tetraploid wheat population (AM population) containing 121 F_8 recombinant inbred lines (RILs, including parents) derived from a Chinese landrace 'Ailanmai' (AL, *T. turgidum* L. cv. Ailanmai, 2n=28, AABB) and a wild emmer accession (LM001, *T. turgidum* subsp. *dicoccoides*) was used in this study. They were collected and preserved by Triticeae Research Institute, Sichuan Agricultural University. The spikes of AL and LM001 were shown in Fig. 1.

Trait measurement and data analysis

Trait measurement was conducted from six field environments for AM RILs: Chongzhou (103° 38′ E, 30° 32′ N) in 2017, 2018, 2019, and 2020 (E_1, E_2, E_3, and E_4), Wenjiang (103° 51′ E, 30° 43′ N) in 2020 (E_5), and Ya'an (103° 0′ E, 29° 58′ N) in 2020 (E_6).

Field experiments were carried out in a randomized complete block design with two replications and were managed in accord with the conventional practices of wheat production. Each plot for a single line was space-planted (0.1-m) in a single 1.5-m row with a 0.3-m of row spacing (Ma et al. 2019b). The measuring methods of partial agronomic traits were similar to Liu et al. (2020a): SNS was measured by calculating the spikelet number of main-spike; PH was determined by the distance from the soil

132 surface to the tip of main-spike (excluding awns); PTN was represented by the
133 number of productive tiller per plant; SL was counted by the length from the base to
134 the tip of main-spike (excluding awns); KNS was measured as the kernel number of
135 main-spike; TKW was represented by 1000 times of the average kernel weight of
136 main-spike. AD was measured from the sowing date to the date that half of the plants
137 of each line flowered (Ma et al. 2019a). SEL was measured as the distance from the
138 base of the spike to the petiole of the flag leaf (Tao et al. 2019). At least three
139 randomly selected plants with consistent growth status were measured for the above
140 traits and averaged for further analysis. The detailed environments for measuring
141 these agronomic traits were listed in Table S1.

142 The basic analysis of the phenotypic data including Pearson's correlation, frequency
143 distribution, standard error, and Student's *t*-test ($P < 0.05$) was performed using IBM
144 SPSS Statistics 25 (http://en.wikipedia.org/wiki/SPSS). The broad-sense heritability
145 (H^2) and best linear unbiased prediction (BLUP) of agronomic traits from different
146 environments were calculated by SAS version 8.0 (https://www.sas.com).

147 **Genetic map construction**

148 High-quality genomic DNA was isolated from fresh leaves of AM RILs following the
149 instructions of Plant Genomic DNA Kit (Tiangen Biotech, Beijing China). The DNA
150 of each line was genotyped using the wheat 55K SNP array from CapitalBio
151 Technology (Beijing, China).

152 The construction processes of genetic map were consistent with the methods of Liu et
153 al. (2018). Specifically, markers from the group of Poly High Resolution in the wheat
154 55K SNP array were retained for the next analysis. Further, markers showing minor
155 allele frequency (< 0.3) among the AM RILs were removed, and markers from the D
156 genome were also deleted. According to their separation patterns in AM RILs, the
157 parameters 'Distortion value' and 'Missing rate' were set as 0.01 and 20%,
158 respectively. The remaining SNP markers were analyzed using the BIN function of

159 IciMapping 4.1 (http://www.isbreeding.net/). Only the marker with 'deleted = 0' from
160 each bin (bin marker) was selected to construct genetic maps. The bin markers were
161 sorted with Kosambi mapping function in JoinMap 4.0
162 (https://www.kyazma.nl/index.php/JoinMap/) and the minimum LOD value was set as
163 5. The genetic maps were drawn using MapChart 2.3.2
164 (http://www.biometris.nl/uk/Software/MapChart/). The syntenic relationships between
165 the genetic and physical maps of bin markers were further carried out by Strawberry
166 Perl 5.24.0.1 (http://perldoc.perl.org/perlintro.html).

167 **QTL analysis**

168 QTL analysis for SNS was performed using the inclusive composite interval mapping
169 (ICIM) in the Biparental Populations (BIP) module of IciMapping 4.1, and the
170 minimal LOD score was set as 2.5. The QTL-by-Environment interaction was
171 analyzed by the multi-environment trials (MET) pattern of IciMapping 4.1.

172 QTL were named according to the provision of Genetic Nomenclature
173 (http://wheat.pw.usda.gov/ggpages/wgc/98/Intro.htm). 'Sns' and 'sau' represented
174 'spikelet number per spike' and 'Sichuan Agricultural University', respectively.
175 Besides, we added the RILs' name 'AM' to QTL's name to distinguish them from
176 others reported previously.

177 The sequences of SNP markers were blasted against the wild emmer
178 (https://www.dropbox.com/sh/3dm05grokh10nbv/AAC3wv1YmAher8fY0srX3gX9a?
179 dl=0%22) (Avni et al. 2017) and common wheat genotype 'Chinese Spring' (CS)
180 genomes (IWGSC RefSeq v1.0; https://urgi.versailles.inra.fr/download/iwgsc/) to get
181 their physical positions. Predicted genes mapped between the flanking markers were
182 gained from the Triticeae Multi-omics Center (http://202.194.139.32/), and their
183 annotation and function were further analyzed using UniProt
184 (http://www.uniprot.org/).

Results

SNP markers and genetic map

As suggested by the Affymetrix Company, the probes from the group of Poly High Resolution with high probability should be reserved. Thus, we retained markers from A and B genome with minor allele frequency (> 0.3) among the SNP markers from the group of Ploy High Resolution. Finally, 7901 SNP markers were classified into 1192 bins, and one marker from each bin was screened to construct the genetic map. The linkage analysis results revealed that 1150 bin markers were mapped on the 15 genetic maps. Subsequently, 6542 co-segregated SNP markers were integrated into the genetic map based on the bin information.

The 1150 bin markers were mapped on 15 linkage groups spanning 2411.78 cM for the 14 chromosomes in tetraploid wheat, and one linkage group was constructed each for all chromosomes except chromosome 3B for which two were obtained (Table 1; Table S2). The average distance of bin markers ranged from 1.09 cM (4B) to 3.64 cM (3B2), with an average density of one bin marker per 2.10 cM (Table 1; Table S2). The lengths of genetic maps ranged from 49.69 cM (3B1) to 225.06 cM (5A) (Table 1; Table S2). Among the 1150 bins, 450 bins contained only one marker, the largest bin included 561 markers on chromosome 2A (Table S3).

The mapped markers (including bin markers and co-segregated markers) ranged from 37 on chromosome 3B1 to 944 on chromosome 2A. What's more, 56% of the mapped markers were distributed on A genomes, and 44% of those were mapped on B genomes (Table 1; Table S3).

Comparison of genetic and physical maps

Based on the sequences of SNP markers, the 6542 mapped markers were blasted against wild emmer and CS reference genomes to get their physical positions, respectively (Table S3). Subsequently, we compared the genetic and physical

chromosomal locations of 1150 bin markers in the wild emmer genome: 35 (3.04%) bin markers showed inconsistent chromosomal locations, 49 (4.26%) bin markers were mapped on unknown chromosomes, and the rest of bin markers were well matched (Table S3; Fig. 2; Fig. 3).

Similarly, we also compared the genetic and physical chromosomal locations of all the 6542 mapped markers in the wild emmer genome. The results showed that 125 (1.91%) markers were mapped on the unknown chromosomes, and 213 (3.26%) markers were mapped on inconsistent chromosomal locations (Table S3). The genetic and physical location of each remaining marker was identical and had roughly the same SNP order (Table S3; Fig. S1).

Among the 6542 mapped markers, the physical chromosomal locations of 295 (4.51%) markers were inconsistent on wild emmer and CS reference genomes, and those of the remaining markers (6247, 95.49%) showed good consistencies.

Phenotypic variation

The SNS of AL and LM001 in six environments ranged from 25.00 to 27.00 and from 23.33 to 26.00, respectively, and that of AM RILs from 15.33 to 34.00 (Table 2). The broad-sense heritability (H^2) of SNS was 0.82 (Table 2), indicating that the SNS trait of the AM population was mainly controlled by genetic factors than environmental factors. Significant correlation coefficients ranging from 0.500 to 0.761 of SNS between six environments were detected (Table 3). In addition, the frequency distribution of SNS indicated that SNS was polygenic inheritance in multiple environments (Fig. S2).

Pearson's correlations between SNS and other agronomic traits

Pearson's correlations were analyzed between SNS and seven other agronomic traits based on the BLUP values. SNS was significantly and positively correlated with PH, AD, SL, SEL, KNS, and TKW (Table 4). No significant correlation was observed

between SNS and PTN (Table 4).

Analysis of SNS QTL

A total of fourteen QTL were identified in the AM RIL population. They were distributed on chromosomes 1A (1 QTL), 3A (1), 5A (2), 6A (1), 2B (3), 3B (2), 4B (1), 5B (2) and 6B (1), with LOD scores from 2.53 to 13.28 and explained 4.23-27.26% of the phenotypic variation (Table 5). The positive alleles of eight QTL were from AL and those of the other six were contributed by LM001. Four QTL were detected in at least two environments and the other ten only in a single environment (Table 5).

QSns.sau-AM-5A.2 was identified in two environments and located in a 19.10 cM region between *AX-108790581* and *AX-111596791*. It accounted for 6.69-14.34% of the phenotypic variation (Table 5). AM RILs were divided into two categories based on the genotype of this QTL's flanking markers. The SNS of the lines with the positive allele was significantly higher than that with the negative allele from *QSns.sau-AM-5A.2* (Fig. 4a).

QSns.sau-AM-2B.3 was stably identified in all environments and explained 9.64-27.26% of the phenotypic variation. It was located in a 1.79 cM region between *AX-111626925* and *AX-111588559* (Table 5). The additive effect of *QSns.sau-AM-2B.3* was negative, indicating that the increasing-SNS allele was contributed by LM001 (Table 5; Fig. 4b).

QSns.sau-AM-3B.1 and *QSns.sau-AM-3B.2* were detected in two and four environments, respectively. They explained up to 18.06% and 13.74% of the phenotypic variation (Table 5). The positive alleles of *QSns.sau-AM-3B.1* and *QSns.sau-AM-3B.2* were both from AL. As expected, lines carrying the positive allele of either *QSns.sau-AM-3B.1* or *QSns.sau-AM-3B.2* had higher SNS than those with the negative allele (Fig. 4c, d).

263 Forty-two QTL were identified in the QTL-by-Environment interaction analysis
264 (Table S4). Nine of them, including *QSns.sau-AM-5A.2*, *QSns.sau-AM-2B.3*,
265 *QSns.sau-AM-3B.1*, and *QSns.sau-AM-3B.2*, were the same as detected in individual
266 environment analysis. These results indicated that these nine QTL were stably
267 expressed for SNS.

268 **Effects of two major QTL on increasing SNS**

269 In this study, two major and stably expressed QTL (i.e. *QSns.sau-AM-2B.3* and
270 *QSns.sau-AM-3B.2*) were identified for SNS in more than three environments. Their
271 effects on increasing SNS were further revealed based on the genotype of flanking
272 markers by Student's *t*-test (Fig. 5).

273 Compared with the lines carried the negative alleles from two major QTL, the lines
274 with the positive allele of *QSns.sau-AM-2B.3* significantly increased SNS by 8.23%;
275 those with the positive allele of *QSns.sau-AM-3B.2* significantly increased SNS by
276 6.52%; the combined effects of two major QTL significantly increased SNS by
277 17.47% (Fig. 5). The results showed that *QSns.sau-AM-2B.3* had the largest effect on
278 increasing SNS among the two major QTL, and there were no significant differences
279 between the effects of *QSns.sau-AM-2B.3* and *QSns.sau-AM-3B.2* on increasing SNS
280 (Fig. 5). Compared with the lines which just carried the positive allele from *QSns.sau-*
281 *AM-2B.3* or *QSns.sau-AM-3B.2*, the combined effects of *QSns.sau-AM-2B.3* and
282 *QSns.sau-AM-3B.2* increased SNS by 8.53% and 10.28%, respectively (Fig. 5).

283 **Effects of two major QTL on other agronomic traits**

284 To analyze the effects of the two major QTL (i.e. *QSns.sau-AM-2B.3* and *QSns.sau-*
285 *AM-3B.2*) on other agronomic traits, AM RILs were divided into two categories based
286 on the genotype of flanking markers of two major QTL: lines with the positive alleles
287 of two major QTL and lines carried the negative alleles from them. The analysis
288 results between the two categories showed that the combined effects *QSns.sau-AM-*

289 *2B.3* and *QSns.sau-AM-3B.2* significantly influenced the SL, SEL, and KNS, but not
290 significantly affected PH, AD, PTN, and TKW (Fig. 6).

291 **Discussion**

292 **The feasibility of wheat 55K SNP array in QTL mapping of tetraploid wheat**

293 The wheat 55K SNP array has been widely used for genotyping and QTL
294 identification mostly in hexaploid common wheat (Ren et al. 2018; Liu et al. 2020b;
295 Ma et al. 2020). In the current study, the wheat 55K SNP array was employed for
296 genotyping a tetraploid wheat RIL population and a high-quality genetic linkage map
297 was constructed. Further, two major QTL for SNS were detected. These results
298 confirmed the feasibility of wheat 55K SNP array in the genetic mapping of tetraploid
299 wheat.

300 **Exploration of loci for SNS from tetraploid wheat species**

301 Previous studies discussed the SNS in tetraploid wheat at the QTL level. Peng et al.
302 (2001) identified QTL for SNS on chromosomes 1B, 2A, 5A, and 6B in an F_2 wild
303 emmer × durum wheat population with a total of 49.3% phenotypic variation
304 explained. Four QTL for SNS were detected on 1B, 3B, 7A, and 7B chromosomes in
305 a tetraploid wheat RIL population developed from the cross between durum wheat and
306 cultivated emmer wheat (Faris et al. 2014a). *QSpn.fcu-2A* was detected from durum
307 wheat Langdon × Langdon-wild emmer wheat substitution lines population and
308 explained 19.4% of the phenotypic variation (Faris et al. 2014b). *QSpn.fcu-1B* and
309 *QSpn.fcu-5A* were identified with 5.1 and 11.4 of LOD scores, respectively, in a
310 durum wheat × cultivated emmer population (Sharma et al. 2019). These previous
311 reports enhanced our understanding of the SNS in tetraploid wheat.

312 In the current research, the positive alleles of major and stably expressed QTL
313 *QSns.sau-AM-2B.3* and *QSns.sau-AM-3B.2* were contributed by wild emmer wheat
314 and Chinese landrace 'Ailanmai', respectively. Compared with lines possessed the

315 negative alleles from two major QTL, the combined effects of two major QTL
316 significantly increased SNS by 17.47% (Fig. 5). We considered that *QSns.sau-AM-*
317 *2B.3* and *QSns.sau-AM-3B.2* identified in tetraploid wheat species had higher
318 application potential for wheat yield improvement.

319 **Comparison of the major QTL identified for SNS with previous studies**

320 No significant differences for SNS were detected between the parents AL and LM001
321 in multiple environments (Table 2). However, the phenotypic data of SNS in six
322 environments showed approximately normal distribution (Fig. S2), and we further
323 identified two major and stably expressed QTL for SNS. The possible explanation for
324 this phenomenon was that transgressive inheritance occurred in progenies and resulted
325 in the bidirectional segregation of SNS. It was deduced that several genes controlling
326 SNS might be inhibited each other in a given parental genotype resulting in the
327 absence of the corresponding phenotype in the parents. However, the single locus
328 produced by genetic recombination between parental genotypes displayed an obvious
329 phenotype in progenies without interference by other loci that control the same traits.
330 Hence, we could identify major SNS loci in the AM RIL population. This was not
331 uncommon in the past studies of QTL identification based on RIL populations (Liu et
332 al. 2020a; Shang et al. 2020).

333 To further identify whether *QSns.sau-AM-2B.3* and *QSns.sau-AM-3B.2* were novel
334 QTL, we physically located previous SNS QTL on chromosome 2B and 3B in wild
335 emmer and CS reference genomes (Table S5). *QSns.sau-AM-2B.3* was physically
336 located on chromosome arm 2BL at 714.47-717.09 Mbp (Fig. 7a). Some QTL for
337 SNS were detected on chromosome arm 2BS in previous studies, but none was
338 reported on 2BL (Table S5). For example, *Qspn-2007* was identified on chromosome
339 2B with the closest marker *Xgwm429* (73.62 Mbp) (Manickavelu et al. 2011).
340 *QFsn.sdau-2B-1* was located on chromosome arm 2BS and explained up to 28.43% of
341 the phenotypic variation (Deng et al. 2017). Xie et al. (2015) detected three QTL for
342 SNS on chromosome arm 2BS in an F_5 RIL population. And some genes affected SNS

were detected on chromosome arm 2BS, such as *Ppd-B1* (Mohler et al. 2004) and *WFZP-2B* (Dobrovolskaya et al. 2015).

QSns.sau-AM-3B.2 was physically located on chromosome arm 3BS at 62.41-65.16 Mbp (Fig. 7b). In previous studies, Azadi et al. (2015) detected four QTL for SNS on chromosome arm 3BL. *QSpn.fcu-3B* was located at 74.28-120.61 Mbp with flanking markers *IWA3716* and *IWA6201* (Faris et al. 2014a). Cui et al. (2012) identified two QTL named *QSpn.WJ.3B.1* and *QSpn.WY.3B.1* all closely linked to the locus *Xgwm566* (77.72 Mbp).

Comparison of physical positions of *QSns.sau-AM-2B.3* and *QSns.sau-AM-3B.2* with those reported previously showed that they were not overlapped with known SNS QTL, further indicating that they were probably novel QTL controlling SNS in tetraploid wheat.

Predicted genes in the physical intervals of major QTL

QSns.sau-AM-2B.3 was physically located in 709.43-712.30 Mbp and 714.47-717.09 Mbp of wild emmer and CS reference genomes, respectively (Fig. 7a). In the corresponding intervals, there were 32 and 27 predicted genes, respectively (Table S6). Additionally, 18 functional orthologs were found among the predicted genes of *QSns.sau-AM-2B.3* (Table S6). *QSns.sau-AM-3B.2* was detected in 70.92-73.35 Mbp and 62.41-65.16 Mbp of wild emmer and CS reference genomes, respectively, and there were 24 functional orthologs (Table S7; Fig. 7b).

Of these orthologs, *TRIDC2BG075100* and *TRIDC3BG013290* were members of the F-box protein family. Previous studies showed that the F-box family protein played vital roles in the control of flowering time, floral organ development, and cell proliferation (Samach et al. 1999; Nelson et al. 2000; Xu et al. 2016). *TRIDC2BG075120* encoded an IQ-domain 32 protein that cooperated with calmodulin to regulate the basic defense response and the growth of plants (Cornelia et al. 2013).

369 *TRIDC2BG075260* encoded a serine hydroxymethyltransferase (SHMT) which was a
370 key enzyme in plant photorespiration. Lack of SHMT could cause severe growth
371 delay and weaken resistance to abiotic stress (Beckmann et al. 1997).
372 *TRIDC3BG013250* was a member of Receptor-like protein kinases (RLKs). And
373 RLKs were known to be involved in signal transduction, plant growth and
374 development (Walker 2010). The above-mentioned genes all played an important role
375 in plant growth and development, which might participate in the formation of wheat
376 spikelet and affect SNS. In general, these results provided the foundation for our
377 following work in fine mapping and gene cloning of major QTL.

378 **Significant correlations between SNS and other agronomic traits**

379 A significant and positive correlation was observed between SNS and SL (Table 4).
380 We could understand it as the increase in SL required a longer spike development
381 stage in combination with optimal temperature and light promoting the germination of
382 more spikelets in wheat (Rawson and Richards 1993; Shaw et al. 2013). SNS was
383 significantly and positively correlated with PH in our results (Table 4), which was
384 supported by the conclusions from Ajmal et al. (2009) and Wu et al. (2012). We
385 speculated that SL was part of PH, and the higher plant had a long spike with more
386 spikelets (Yao et al. 2011). A significant and positive relationship was detected
387 between SNS and AD (Table 4), confirming the results by Ma et al. (2019a). Previous
388 studies suggested that the wheat plants with later flowering dates might produce
389 longer spikes with more spikelets (Shaw et al. 2013; Kamran et al. 2014; Boden et al.
390 2015). These results indicated that AD played an important role in the formation of
391 spikelet. On the whole, floret fertility determined the KNS in wheat, and thus more
392 spikelets would produce more fertile florets accompanied with an increase of KNS
393 (Gao et al. 2019; Sakuma et al. 2019). This was likely the reason why SNS was
394 significantly and positively correlated with KNS (Table 4).

395 It was generally believed that a negative correlation should be observed between SNS
396 and TKW (Li et al. 2007; Ma et al. 2019a) due to a source limitation during kernel

filling or the existence of more kernels with lower KW in the distal positions of the spike (Quintero et al. 2018). Previous studies also suggested that SNS was negatively correlated with SEL because of the competition for assimilating products between SNS and SEL (Miralles et al. 1998; Bancal 2008; Li et al. 2020). The above conclusions were inconsistent with our study that SNS was significantly and positively correlated with TKW and SEL (Table 4). Our further results also revealed there were significant differences in the SEL between two types (lines with or without the positive alleles from major QTL) (Fig. 6e). It probably indicated that the loci controlling SNS played an individual role without interaction with SEL. According to the previous studies, SEL had a special function in photosynthesis and the storage of nutrients and water, hence, a longer SEL would be more conducive to ventilation and transporting more nutrients and water to kernels (Bridgemohan and Bridgemohan 2014; Ávila-Lovera et al. 2017), finally likely increasing the KW. Thus, SNS was significantly and positively correlated with SEL and TKW in the current study. These conclusions were helpful for us to comprehensively consider the complex relationship in agronomic traits and might provide new insights into wheat yield improvement.

Notes

Acknowledgments

This work is supported by the National Natural Science Foundation of China (31971937 and 31970243), the Key Research and Development Program of Sichuan Province (2018NZDZX0002), the Applied Basic Research Programs of Science and Technology Department of Sichuan Province (2020YJ0140), and the Key Projects of Scientific and Technological Activities for Overseas Students of Sichuan Province. We thank the anonymous referees for critical reading and revising this manuscript.

Author contribution statement

ZQM and JZ conducted the study and drafted this manuscript. JTW and JGZ participated in phenotype measurement and data analysis. QX and HPT helped with

field work and data analysis. YM, QTJ, and YXL participated in data collection and analysis. GYC, JRW, PFQ, ZEP, and GDC did QTL analysis and manuscript revision. YMW and YLZ discussed results and revised the manuscript. XJL guided the study and revised the manuscript. JM designed the experiments, guided the entire study, participated in data analysis, wrote and extensively revised this manuscript. All authors participated in the research and approved the final manuscript.

Compliance with ethical standards

Conflict of interest

All authors declare that there is no conflict of interest.

Ethical standards

All experiments and data analyses were conducted in Sichuan. All authors contributed to the study and approved the final version for submission. The manuscript has not been submitted to any other journal.

References

Ajmal S, Zakir N, Mujahid M (2009) Estimation of genetic parameters and character association in wheat. J Agric Biol Sci 1:15-18

Ávila-Lovera E, Zerpa AJ, Santiago LS (2017) Stem photosynthesis and hydraulics are coordinated in desert plant species. New Phytol 216:1119-1129

Avni R, Nave M, Barad O, Baruch K, Twardziok S, Gundlach H, Hale I, Mascher M, Spannagl M, Wiebe K, Jordan K, Golan G, Deek J, Ben-Zvi B, Ben-Zvi G, Himmelbach A, MacLachlan R, Sharpe A, Fritz A, Ben-David R, Budak H, Fahima T, Korol A, Faris J, Hernandez A, Mikel M, Levy A, Steffenson B, Maccaferri M, Tuberosa R, Cattivelli L, Faccioli P, Ceriotti A, Kashkush K, Pourkheirandish M, Komatsuda T, Eilam T, Sela H, Sharon A, Ohad N, Chamovitz D, Mayer K, Stein N, Ronen G, Peleg Z, Pozniak C, Akhunov E, Distelfeld A (2017) Wild emmer genome architecture and diversity elucidate wheat evolution and domestication. Science 357:93-97

Azadi A, Mardi M, Hervan EM, Mohammadi SA, Moradi F, Tabatabaee MT, Pirseyedi SM, Ebrahimi M, Fayaz F, Kazemi M, Ashkani S, Nakhoda B, Mohammadi Nejad G (2015) QTL mapping of yield and yield components under normal and salt-stress conditions in bread wheat (*Triticum aestivum* L.). Plant Mol Biol Rep 33:102-120

Bancal P (2008) Positive contribution of stem growth to grain number per spike in

wheat. Field Crop Res 105:27-39
Beckmann K, Dzuibany C, Biehler K, Fock H, Hell R, Migge A, Becker TW (1997) Photosynthesis and fluorescence quenching, and the mRNA levels of plastidic glutamine synthetase or of mitochondrial serine hydroxymethyltransferase (SHMT) in the leaves of the wild-type and of the SHMT-deficient stm mutant of *Arabidopsis thaliana* in relation to the rate of photorespiration. Planta 202:379-386
Boden SA, Cavanagh C, Cullis BR, Ramm K, Greenwood J, Jean Finnegan E, Trevaskis B, Swain SM (2015) *Ppd-1* is a key regulator of inflorescence architecture and paired spikelet development in wheat. Nat Plants 1:14016
Bridgemohan P, Bridgemohan RSH (2014) Evaluation of anti-lodging plant growth regulators on the growth and development of rice (*Oryza sativa*). J Cereals Oilseeds 5:12-16
Cavanagh CR, Chao S, Wang S, Huang BE, Stephen S, Kiani S, Forrest KL, Saintenac C, Brownguedira G, Akhunova A (2013) Genome-wide comparative diversity uncovers multiple targets of selection for improvement in hexaploid wheat landraces and cultivars. P Natl Acad Sci USA 110:8057-8062
Chen Z, Cheng X, Chai L, Wang Z, Du D, Wang Z, Bian R, Zhao A, Xin M, Guo W, Hu Z, Peng H, Yao Y, Sun Q, Ni Z (2020) Pleiotropic QTL influencing spikelet number and heading date in common wheat (*Triticum aestivum* L.). Theor Appl Genet 133:1825-1838
Cornelia F, Annette K, Stefan H, Petra D (2013) An IQ domain mediates the interaction with calmodulin in a plant cyclic nucleotide-gated channel. Plant Cell Physiol 54:573-584
Crossa J, Jarquin D, Franco J, Perezrodriguez P, Burgueno J, Saintpierre C, Vikram P, Sansaloni C, Petroli C, Akdemir D (2016) Genomic prediction of gene bank wheat landraces. G3-Gens Genom Genet 6:1819-1834
Cui F, Ding A, Li J, Zhao C, Wang L, Wang X, Qi X, Li X, Li G, Gao J, Wang H (2012) QTL detection of seven spike-related traits and their genetic correlations in wheat using two related RIL populations. Euphytica 186:177-192
Deng Z, Cui Y, Han Q, Fang W, Li J, Tian J (2017) Discovery of consistent QTLs of wheat spike-related traits under nitrogen treatment at different development stages. Front Plant Sci 8:2120
Dixon LE, Greenwood JR, Bencivenga S, Zhang P, Cockram J, Mellers G, Ramm K, Cavanagh C, Swain SM, Boden SA (2018) *TEOSINTE BRANCHED1* regulates inflorescence architecture and development in bread wheat (*Triticum aestivum*). Plant Cell 30:563-581
Dobrovolskaya O, Pont C, Sibout R, Martinek P, Badaeva E, Murat F, Chosson A, Watanabe N, Prat E, Gautier N, Gautier V, Poncet C, Orlov YL, Krasnikov AA, Bergès H, Salina E, Laikova L, Salse J (2015) *FRIZZY PANICLE* drives supernumerary spikelets in bread wheat. Plant Physiol 167:189-199
Faris JD, Zhang Q, Chao S, Zhang Z, Xu SS (2014a) Analysis of agronomic and domestication traits in a durum × cultivated emmer wheat population using a

high-density single nucleotide polymorphism-based linkage map. Theor Appl Genet 127:2333-2348

Faris JD, Zhang Z, Garvin DF, Xu SS (2014b) Molecular and comparative mapping of genes governing spike compactness from wild emmer wheat. Mol Genet Genomics 289:641-651

Gao X, Wang N, Wang X, Zhang X (2019) Architecture of wheat inflorescence: insights from rice. Trends Plant Sci 24(9):802-809

Kamran A, Iqbal M, Spaner D (2014) Flowering time in wheat (*Triticum aestivum* L.): a key factor for global adaptability. Euphytica 197:1-26

Klymiuk V, Yaniv E, Huang L, Raats D, Fatiukha A, Chen S, Feng L, Frenkel Z, Krugman T, Lidzbarsky G (2018) Cloning of the wheat *Yr15* resistance gene sheds light on the plant tandem kinase-pseudokinase family. Nat Commun 9:3735

Kuzay S, Xu Y, Zhang J, Katz A, Pearce S, Su Z, Fraser M, Anderson JA, Brown-Guedira G, DeWitt N, Peters Haugrud A, Faris JD, Akhunov E, Bai G, Dubcovsky J (2019) Identification of a candidate gene for a QTL for spikelet number per spike on wheat chromosome arm 7AL by high-resolution genetic mapping. Theor Appl Genet 132:2689-2705

Li C, Tang H, Luo W, Zhang X, Mu Y, Deng M, Liu Y, Jiang Q, Chen G, Wang J, Qi P, Pu Z, Jiang Y, Wei Y, Zheng Y, Lan X, Ma J (2020) A novel, validated, and plant height-independent QTL for spike extension length is associated with yield-related traits in wheat. Theor Appl Genet 133:3381-3393

Li S, Jia J, Wei X, Zhang X, Li L, Chen H, Fan Y, Sun H, Zhao X, Lei T, Xu Y, Jiang F, Wang H, Li L (2007) A intervarietal genetic map and QTL analysis for yield traits in wheat. Mol Breeding 20:167-178

Lin Y, Chen G, Hu H, Yang X, Zhang Z, Jiang X, Wu F, Shi H, Wang Q, Zhou K, Li C, Ma J, Zheng Y, Wei Y, Liu Y (2020) Phenotypic and genetic variation in phosphorus-deficiency-tolerance traits in Chinese wheat landraces. BMC Plant Biol 20:330

Liu H, Ma J, Tu Y, Zhu J, Ding P, Liu J, Li T, Zou Y, Habib A, Mu Y, Tang H, Jiang Q, Liu Y, Chen G, Zheng Y, Wei Y, Lan X (2020a) Several stably expressed QTL for spike density of common wheat (*Triticum aestivum*) in multiple environments. Plant Breeding 139:284-294

Liu J, Luo W, Qin N, Ding P, Zhang H, Yang C, Mu Y, Tang H, Liu Y, Li W, Jiang Q, Chen G, Wei Y, Zheng Y, Liu C, Lan X, Ma J (2018) A 55 K SNP array-based genetic map and its utilization in QTL mapping for productive tiller number in common wheat. Theor Appl Genet 131:2439-2450

Liu J, Tang H, Qu X, Liu H, Li C, Tu Y, Li S, Habib A, Mu Y, Dai S, Deng M, Jiang Q, Liu Y, Chen G, Wang J, Chen G, Li W, Jiang Y, Wei Y, Lan X, Zheng Y, Ma J (2020b) A novel, major, and validated QTL for the effective tiller number located on chromosome arm 1BL in bread wheat. Plant Mol Biol 104:173-185

Longin CFH, Reif JC (2014) Redesigning the exploitation of wheat genetic resources. Trends Plant Sci 19:631-636

Lopes MS, Ibrahim EB, Baenziger PS, Sukhwinder S, Conxita R, Kursad O, Husnu A,

Emel O, Fatih O, Alagu M (2015) Exploiting genetic diversity from landraces in wheat breeding for adaptation to climate change. J Exp Bot 66:3477-3486

Ma J, Ding P, Liu J, Li T, Zou Y, Habib A, Mu Y, Tang H, Jiang Q, Liu Y, Chen G, Wang J, Deng M, Qi P, Li W, Pu Z, Zheng Y, Wei Y, Lan X (2019a) Identification and validation of a major and stably expressed QTL for spikelet number per spike in bread wheat. Theor Appl Genet 132:3155-3167

Ma J, Qin N, Cai B, Chen G, Ding P, Zhang H, Yang C, Huang L, Mu Y, Tang H, Liu Y, Wang J, Qi P, Jiang Q, Zheng Y, Liu C, Lan X, Wei Y (2019b) Identification and validation of a novel major QTL for all-stage stripe rust resistance on 1BL in the winter wheat line 20828. Theor Appl Genet 132:1363-1373

Ma J, Tu Y, Zhu J, Luo W, Liu H, Li C, Li S, Liu J, Ding P, Habib A, Mu Y, Tang H, Liu Y, Jiang Q, Chen G, Wang J, Li W, Pu Z, Zheng Y, Wei Y, Kang H, Chen G, Lan X (2020) Flag leaf size and posture of bread wheat: genetic dissection, QTL validation and their relationships with yield-related traits. Theor Appl Genet 133:297-315

Manickavelu A, Kawaura K, Imamura H, Mori M, Ogihara Y (2011) Molecular mapping of quantitative trait loci for domestication traits and β-glucan content in a wheat recombinant inbred line population. Euphytica 177:179-190

Martínez-Moreno F, Solís I, Noguero D, Blanco A, Özberk İ, Nsarellah N, Elias E, Mylonas I, Soriano JM (2020) Durum wheat in the Mediterranean Rim: historical evolution and genetic resources. Genet Resour Crop Evol 67:1415-1436

Miralles DJ, Katz SD, Colloca A, Slafer GA (1998) Floret development in near isogenic wheat lines differing in plant height. Field Crop Res 59:21-30

Mohler V, Lukman R, Ortiz-Islas S, William M, Worland AJ, van Beem J, Wenzel G (2004) Genetic and physical mapping of photoperiod insensitive gene *Ppd-B1* in common wheat. Euphytica 138:33-40

Nelson DC, Lasswell J, Rogg LE, Cohen MA, Bartel B (2000) *FKF1*, a clock-controlled gene that regulates the transition to flowering in *Arabidopsis*. Cell 101(3):331-340

Peng J, Korol A, Fahima T, Roder M, Li Y, Nevo E (2001) QTLs for agronomic traits in tetraploid wild emmer wheat, *Triticum dicoccoides*. J Sichuan Agric Univ 19(4):317-334 **(in Chinese)**

Quintero A, Molero G, Reynolds MP, Calderini DF (2018) Trade-off between grain weight and grain number in wheat depends on GxE interaction: A case study of an elite CIMMYT panel (CIMCOG). Eur J Agron 92:17-29

Rawson HM, Richards RA (1993) Effects of high temperature and photoperiod on floral development in wheat isolines differing in vernalisation and photoperiod genes. Field Crop Res 32:181-192

Ren T, Hu Y, Tang Y, Li C, Yan B, Ren Z, Tan F, Tang Z, Fu S, Li Z (2018) Utilization of a wheat55K SNP array for mapping of major QTL for temporal expression of the tiller number. Front Plant Sci 9:333

Reynolds M, Bonnett D, Chapman SC, Furbank RT, Manes Y, Mather DE, Parry MAJ (2011) Raising yield potential of wheat. I. Overview of a consortium approach

and breeding strategies. J Exp Bot 62:439-452
Sakuma S, Golan G, Guo Z, Ogawa T, Tagiri A, Sugimoto K, Bernhardt N, Brassac J, Mascher M, Hensel G (2019) Unleashing floret fertility in wheat through the mutation of a homeobox gene. P Natl Acad Sci USA 116:5182-5187
Samach A, Klenz J, Kohalmi S, Risseeuw E, Haughn G, Crosby W (1999) The *UNUSUAL FLORAL ORGANS* gene of *Arabidopsis thaliana* is an F-box protein required for normal patterning and growth in the floral meristem. Plant J 20(4):433-445
Shang Q, Zhang D, Li R, Wang K, Cheng Z, Zhou Z, Hao Z, Pan J, Li X, Shi L (2020) Mapping quantitative trait loci associated with stem-related traits in maize (*Zea mays* L.). Plant Molecular Biology. https://doi.org/10.1007/s11103-020-01062-3
Sharma JS, Running KLD, Xu SS, Zhang Q, Peters Haugrud AR, Sharma S, McClean PE, Faris JD (2019) Genetic analysis of threshability and other spike traits in the evolution of cultivated emmer to fully domesticated durum wheat. Mol Genet Genomics 294:757-771
Shaw LM, Turner AS, Laurence H, Simon G, Laurie DA, Somers DE (2013) Mutant alleles of *Photoperiod-1* in wheat (*Triticum aestivum* L.) that confer a late flowering phenotype in long days. PloS ONE 8(11):e79459
Sthapit SR, Marlowe K, Covarrubias DC, Ruff TM, Eagle JD, McGinty EM, Hooker MA, Duong NB, Skinner DZ, See DR (2020) Genetic diversity in historical and modern wheat varieties of the U.S. Pacific Northwest. Crop Sci. https://doi.org/10.1002/csc2.20299
Tanksley SD, McCouch SR (1997) Seed banks and molecular maps: unlocking genetic potential from the wild. Science 277:1063-1066
Tao Y, Yi X, Lin Y, Wang Z, Wu F, Jiang X, Liu S, Deng M, Ma J, Chen G, Wei Y, Zheng Y, Liu Y (2019) Quantitative trait locus mapping for panicle exsertion length in common wheat using two related recombinant inbred line populations. Euphytica 215:104
Walker JC (2010) Receptor-like protein kinase genes of *Arabidopsis thaliana*. Plant J 3:451-456
Wang R, Liu Y, Isham K, Zhao W, Wheeler J, Klassen N, Hu Y, Bonman JM, Chen J (2018) QTL identification and KASP marker development for productive tiller and fertile spikelet numbers in two high-yielding hard white spring wheat cultivars. Mol Breeding 38:135
Wang Y, Yu H, Tian C, Sajjad M, Gao C, Tong Y, Wang X, Jiao Y (2017) Transcriptome association identifies regulators of wheat spike architecture. Plant Physiol 175:746-757
Wu X, Chang X, Jing R (2012) Genetic insight into yield-associated traits of wheat grown in multiple rain-fed environments. PloS ONE 7(2):e31249
Xie Q, Sean M, Sparkes DL (2015) Spelt as a genetic resource for yield component improvement in bread wheat. Crop Sci 55:2753-2765
Xie W, Nevo E (2008) Wild emmer: genetic resources, gene mapping and potential for wheat improvement. Euphytica 164:603-614
Xu X, Zhang X, Shi Y, Wang H, Feng B, Li X, Huang Q, Song L, Guo D, He Y, Wu J

(2016) A point mutation in an F-box domain-containing protein is responsible for brown hull phenotype in rice. Rice Sci 23:1-8

Yao H, Xie Q, Xue S, Luo J, Lu J, Kong Z, Wang Y, Zhai W, Lu N, Wei R, Yang Y, Han Y, Zhang Y, Jia H, Ma Z (2019) *HL2* on chromosome 7D of wheat (*Triticum aestivum* L.) regulates both head length and spikelet number. Theor Appl Genet 132:1789-1797

Yao J, Ren L, Zhang P, Yang X, Zhou M (2011) Genetic and correlation analysis of plant height and its components in wheat. J Triticeae Crop 31(4):604-610 **(in Chinese)**

Yu J, Zhao Y, Ding M, Yu Z, Jiang Y, Ma W, Rong J (2020) Wild emmer chromosome arm substitution lines: Useful resources for wheat genetic study and breeding. Crop Sci 60:1761-1769

Zhang H, Li Y, Miao L, Wang J, Li C, Yang D, Mao X, Jing R (2019) Transcription factor gene *TaNAC67* involved in regulation spike length and spikelet number per spike in common wheat. Acta Agron Sin 45:1615-1627 **(in Chinese)**

Table 1 Information on SNP markers in the genetic map

Chromosome	Group	Number of bin marker	Number of mapped marker	Length (cM)	cM per bin marker
1A	1	101	586	153.29	1.52
1B	1	69	488	149.34	2.16
2A	1	66	944	161.77	2.45
2B	1	92	423	183.69	2.00
3A	1	99	518	160.97	1.63
3B	1	17	37	49.69	2.92
	2	27	174	98.39	3.64
4A	1	80	282	199.90	2.50
4B	1	77	422	83.69	1.09
5A	1	92	299	225.06	2.45
5B	1	121	675	207.52	1.72
6A	1	60	640	167.00	2.78
6B	1	58	160	162.46	2.80
7A	1	92	395	214.20	2.33
7B	1	99	499	194.81	1.97
A genome	7	590	3664	1282.19	2.17
B genome	8	560	2878	1129.59	2.02
Total	15	1150	6542	2411.78	2.10

Table 2 Phenotypic data and heritability (H^2) of spikelet number per spike (SNS) for the AM population in multiple environments

Environment	Parents		AL × LM001 (AM)			
	AL	LM001	Min-Max	Mean	SD	H^2
E_1	25.00	24.33	20.00-31.67	25.96	2.56	
E_2	26.00	23.33	15.33-33.00	24.41	3.22	
E_3	26.33	26.00	17.00-31.25	24.81	2.80	
E_4	26.00	25.40	18.00-32.00	26.21	2.87	
E_5	27.00	24.60	18.50-31.00	24.99	2.42	
E_6	25.80	25.40	20.00-34.00	26.76	2.69	
BLUP	25.98	24.91	18.89-30.54	25.53	2.09	0.82

BLUP phenotype values based on the best linear unbiased prediction, *SD* standard deviation, H^2 the broad-sense heritability

Table 3 Correlations of spikelet number per spike (SNS) in the AM population between six environments

	E_1	E_2	E_3	E_4	E_5	E_6
E_1	1	0.500**	0.619**	0.645**	0.521**	0.534**
E_2		1	0.666**	0.631**	0.626**	0.648**
E_3			1	0.704**	0.672**	0.622**
E_4				1	0.761**	0.616**
E_5					1	0.662**
E_6						1

**Significance level at $P < 0.01$

Table 4 Correlations between spikelet number per spike (SNS) and other agronomic traits in the AM population

	PH	AD	PTN	SL	SEL	KNS	TKW
SNS	0.320**	0.179*	-0.099	0.672**	0.241**	0.423**	0.198*

PH plant height, *AD* anthesis date, *PTN* productive tiller number, *SL* spike length, *SEL* spike extension length, *KNS* kernel number per spike, *TKW* thousand kernel weight. *Significance level at $P < 0.05$, **Significance level at $P < 0.01$

Table 5 Quantitative trait loci (QTL) for spikelet number per spike (SNS) identified in multiple environments in the AM population

QTL	Env.	Interval (cM)	Left Marker	Right Marker	LOD	PVE (%)	Add
QSns.sau-AM-1A	E_2	148.47-153.29	*AX-110167459*	*AX-110373055*	6.73	14.73	-1.31
QSns.sau-AM-3A	E_4	79.51-91.05	*AX-109418113*	*AX-109284498*	3.03	6.91	0.69
QSns.sau-AM-5A.1	E_2	106.81-107.24	*AX-110428951*	*AX-109898601*	3.26	6.11	-0.85
QSns.sau-AM-5A.2	E_1	116.08-131.93	*AX-108790581*	*AX-111499991*	4.78	14.34	-1.02
	E_3	131.93-135.18	*AX-111499991*	*AX-111596791*	3.17	6.69	-0.74
	BLUP	131.93-135.18	*AX-111499991*	*AX-111596791*	6.09	10.28	-0.67
QSns.sau-AM-6A	E_2	91.51-92.38	*AX-109842268*	*AX-108785002*	3.38	6.62	0.87
QSns.sau-AM-2B.1	E_4	92.48-94.75	*AX-109818835*	*AX-108848446*	3.91	9.31	-0.80
QSns.sau-AM-2B.2	E_5	113.67-114.56	*AX-109421413*	*AX-109506426*	3.81	12.71	-0.74
QSns.sau-AM-2B.3	E_1	127.65-129.44	*AX-111626925*	*AX-111588559*	8.19	20.27	-1.21
	E_2	127.65-129.44	*AX-111626925*	*AX-111588559*	5.00	9.64	-1.04
	E_3	127.65-129.44	*AX-111626925*	*AX-111588559*	10.86	27.26	-1.49
	E_4	127.65-129.44	*AX-111626925*	*AX-111588559*	5.71	14.16	-0.98
	E_5	127.65-129.44	*AX-111626925*	*AX-111588559*	5.88	20.77	-0.93
	E_6	127.65-129.44	*AX-111626925*	*AX-111588559*	4.54	13.90	-0.95
	BLUP	127.65-129.44	*AX-111626925*	*AX-111588559*	13.28	26.50	-1.07
QSns.sau-AM-3B.1	E_4	22.72-42.47	*AX-110399975*	*AX-109050064*	6.36	18.06	1.14
	E_6	22.72-42.47	*AX-110399975*	*AX-109050064*	3.11	9.38	0.81
QSns.sau-AM-3B.2	E_1	48.34-49.69	*AX-109393346*	*AX-110548993*	4.13	9.57	0.85
	E_2	48.34-49.69	*AX-109393346*	*AX-110548993*	4.89	9.32	1.05
	E_3	48.34-49.69	*AX-109393346*	*AX-110548993*	5.28	11.82	1.00
	E_5	48.34-49.69	*AX-109393346*	*AX-110548993*	2.53	8.27	0.60
	BLUP	48.34-49.69	*AX-109393346*	*AX-110548993*	7.81	13.74	0.79
QSns.sau-AM-4B	E_2	68.66-69.11	*AX-111151524*	*AX-109338618*	4.13	7.82	0.96
QSns.sau-AM-5B.1	BLUP	131.85-133.16	*AX-110547223*	*AX-108834482*	3.93	6.38	0.53
QSns.sau-AM-5B.2	E_4	142.38-143.74	*AX-110911600*	*AX-109870696*	2.81	6.41	0.66
QSns.sau-AM-6B	BLUP	123.88-124.75	*AX-108748222*	*AX-86183685*	2.67	4.23	0.43

Env. Environment, *BLUP* phenotype values based on the best linear unbiased prediction, *LOD* logarithm of odds, *PVE* phenotype variance explained, *Add* additive effect, positive values: alleles from AL were increasing the trait score, negative values: alleles from LM001 were increasing the score

Fig. 1 The spikes of AL and LM001 (scale bar = 2 cm)

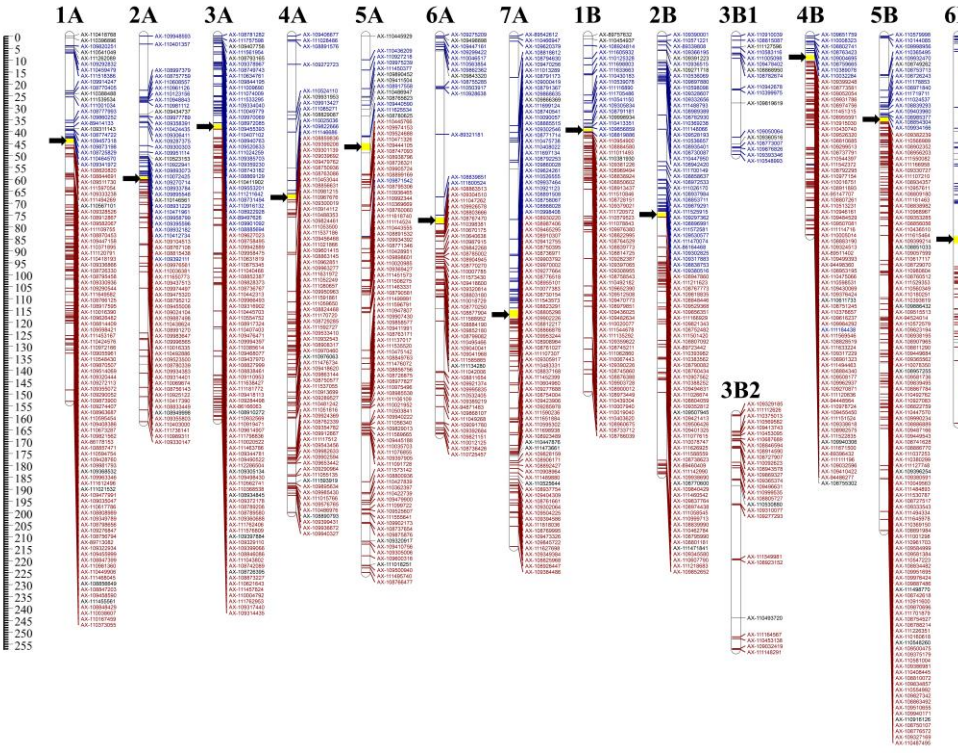

Fig. 2 Distribution information of 1150 bin markers on the genetic maps. The positions of centromeres were indicated by yellow areas and black arrows (Avni et al. 2017). The short arms (blue) and long arms (red) of chromosomes were in the upper and lower parts, respectively. The markers were black indicated that their physical locations were not on the corresponding chromosomes. The names of bin markers were listed on the right side of the chromosomes

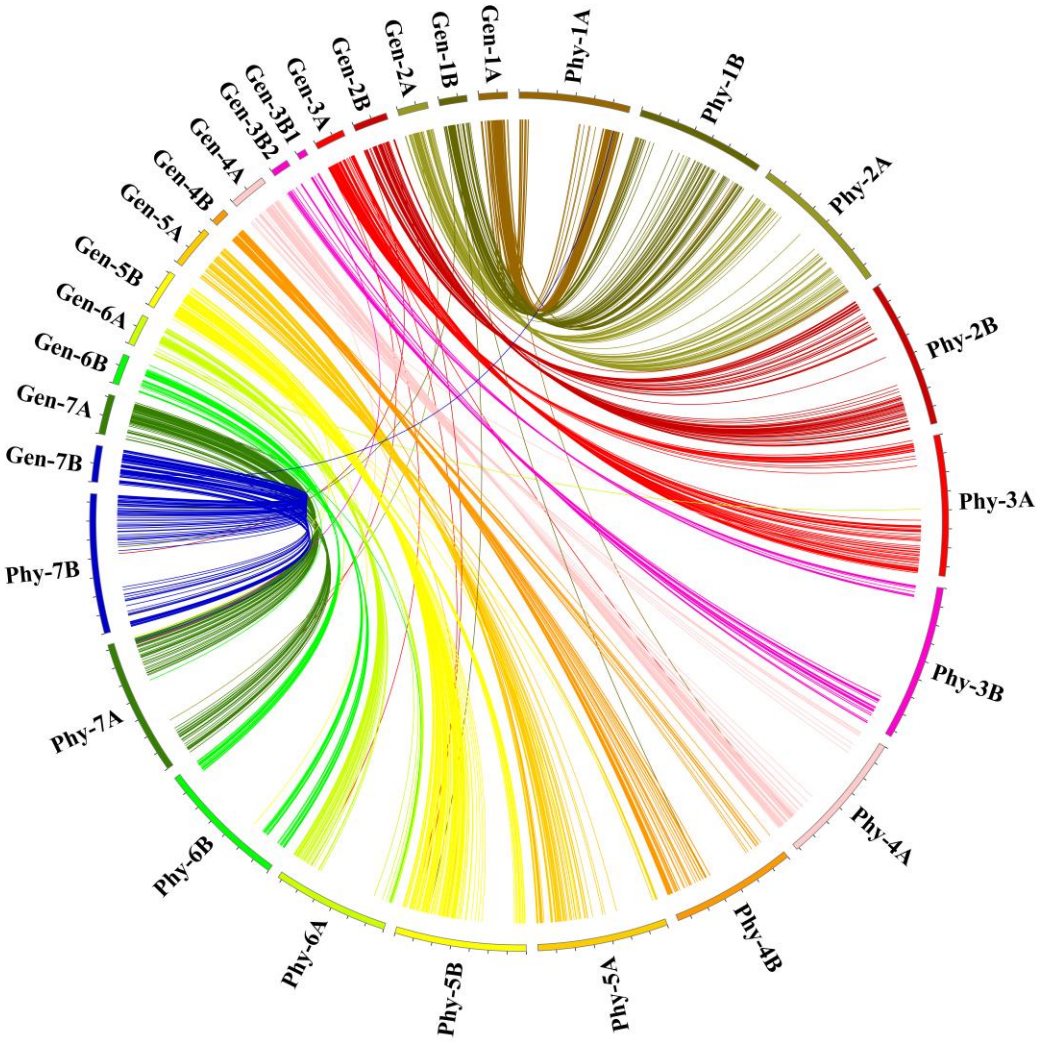

Fig. 3 The syntenic relationships between the genetic and physical maps of bin markers (excluding the 49 bin markers of unknown chromosomes). Gen-1A to Gen-7B represented the 15 chromosomal genetic maps used in the current study; Phy-1A to Phy-7B represented the 14 chromosomal physical maps of wild emmer genome

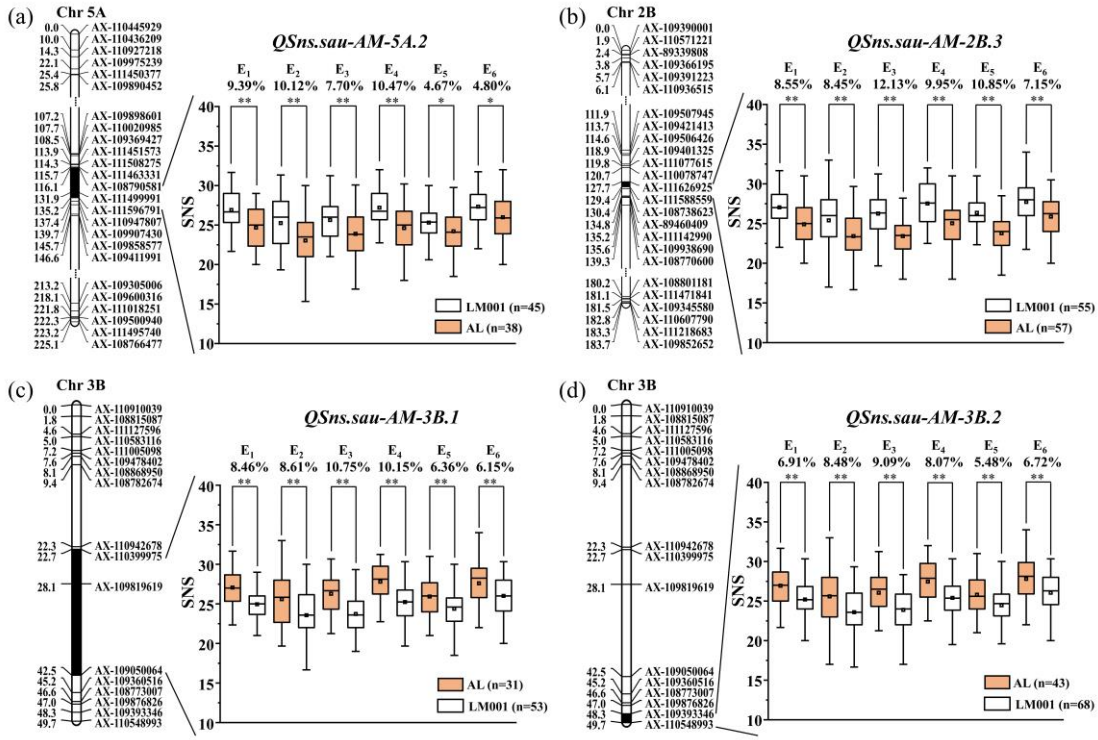

Fig. 4 AM RILs were divided into two categories based on the genotype of flanking markers, and the SNS differences caused by the corresponding QTL were represented in the form of boxplots. Genetic maps of *QSns.sau-AM-5A.2* (**a**), *QSns.sau-AM-2B.3* (**b**), *QSns.sau-AM-3B.1* (**c**), *QSns.sau-AM-3B.2* (**d**) and their effects. *Significance level at $P < 0.05$, **Significance level at $P < 0.01$. The SNS differences between the two categories were marked below the environment names

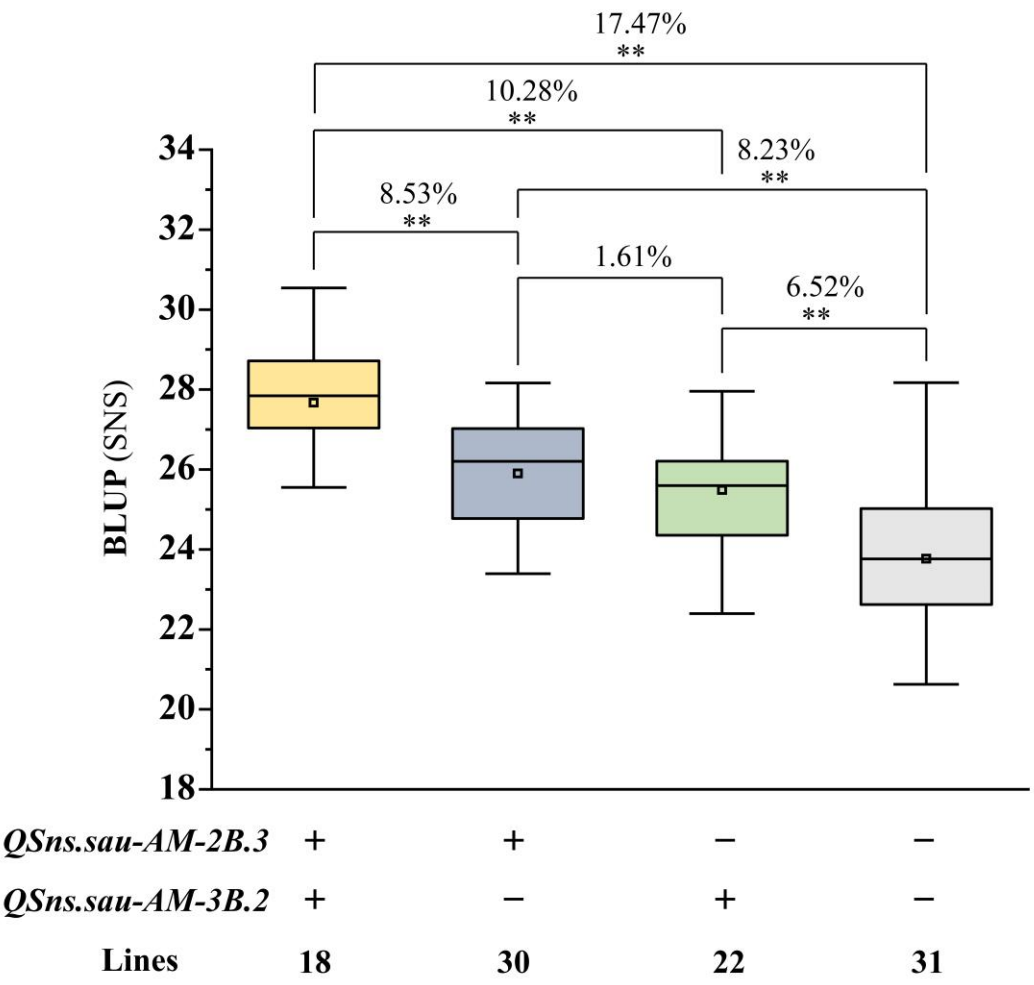

Fig. 5 The effects of different combinations of *QSns.sau-AM-2B.3* and *QSns.sau-AM-3B.2* on increasing SNS in the AM population. '+' and '-' represented lines with and without the positive allele of the corresponding QTL based on the genotype of flanking markers, respectively. *Significance level at $P < 0.05$, **Significance level at $P < 0.01$

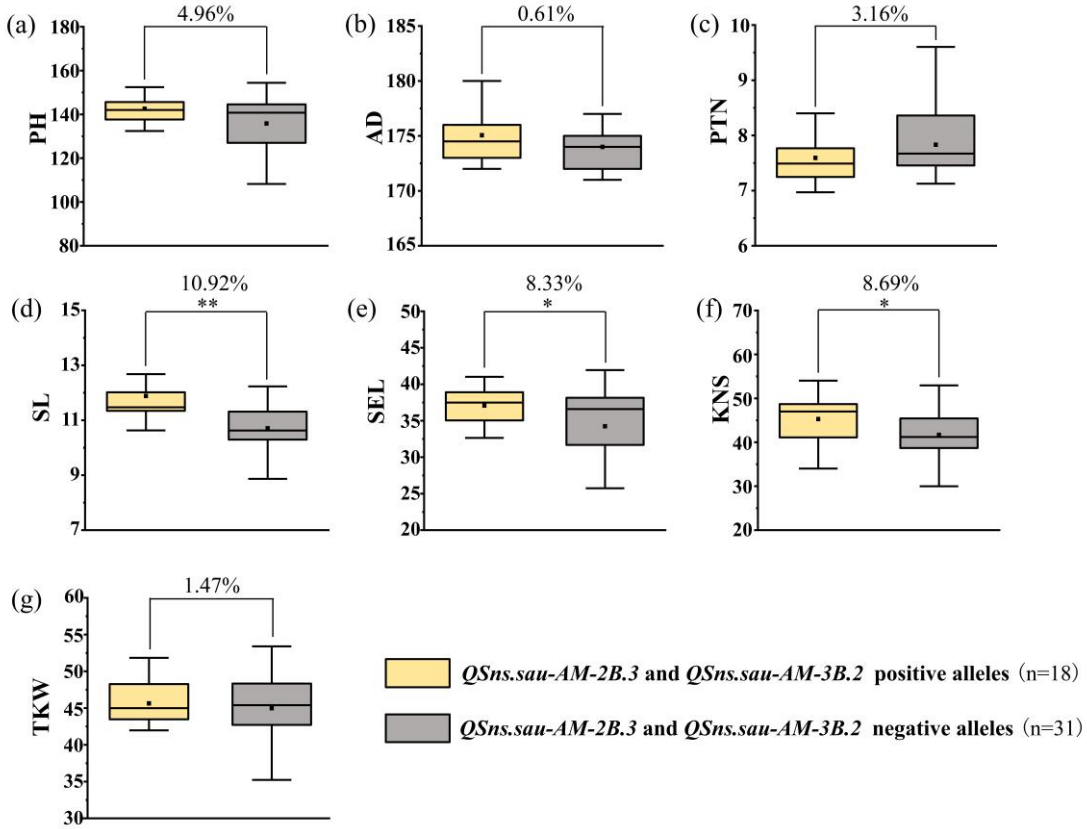

Fig. 6 Student's *t*-test against the two categories of lines from the AM RIL population possessing the positive or negative alleles of both *QSns.sau-AM-2B.3* and *QSns.sau-AM-3B.2* for (**a**) plant height (PH); (**b**) anthesis date (AD); (**c**) productive tiller number (PTN); (**d**) spike length (SL); (**e**) spike extension length (SEL); (**f**) kernel number per spike (KNS); (**g**) thousand kernel weight (TKW). *Significance level at $P < 0.05$, **Significance level at $P < 0.01$. Differences between the two categories of lines were marked above the significance levels

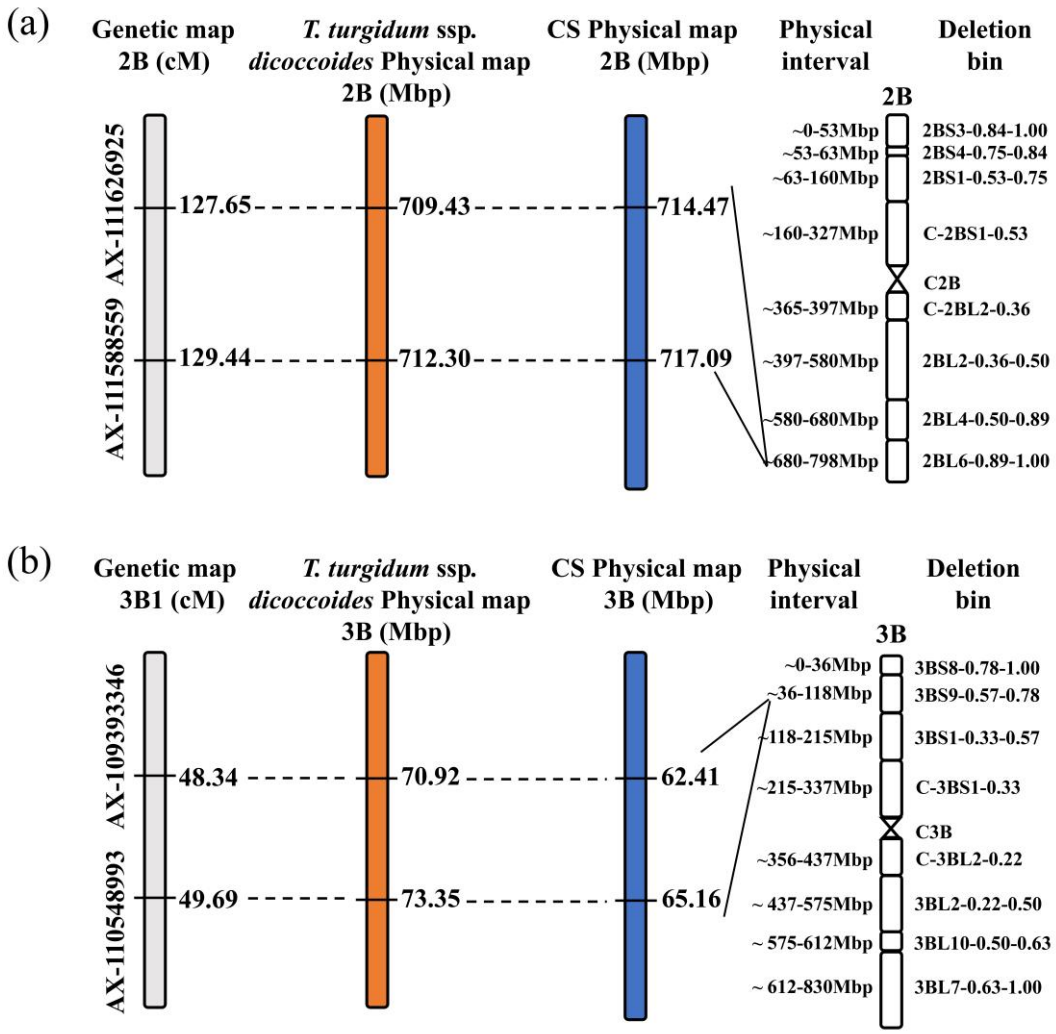

Fig. 7 The physical intervals of *QSns.sau-AM-2B.3* (**a**) and *QSns.sau-AM-3B.2* (**b**)

Supplementary Figures

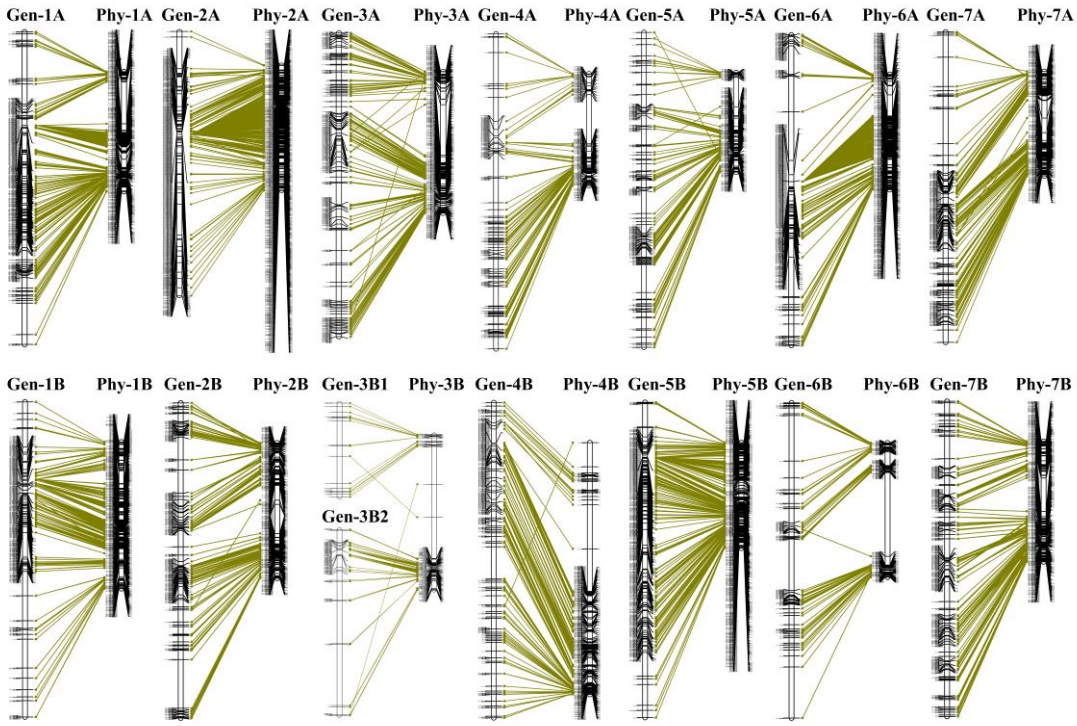

Fig. S1 The syntenic relationships of mapped markers between genetic and physical positions. Excluding 125 markers that had unknown physical chromosomal locations and 213 markers which had inconsistent chromosomal locations between genetic and physical maps. Gen-1A to Gen-7B represented the 15 genetic maps used in the current study; Phy-1A to Phy-7B represented the 14 physical maps of wild emmer genome

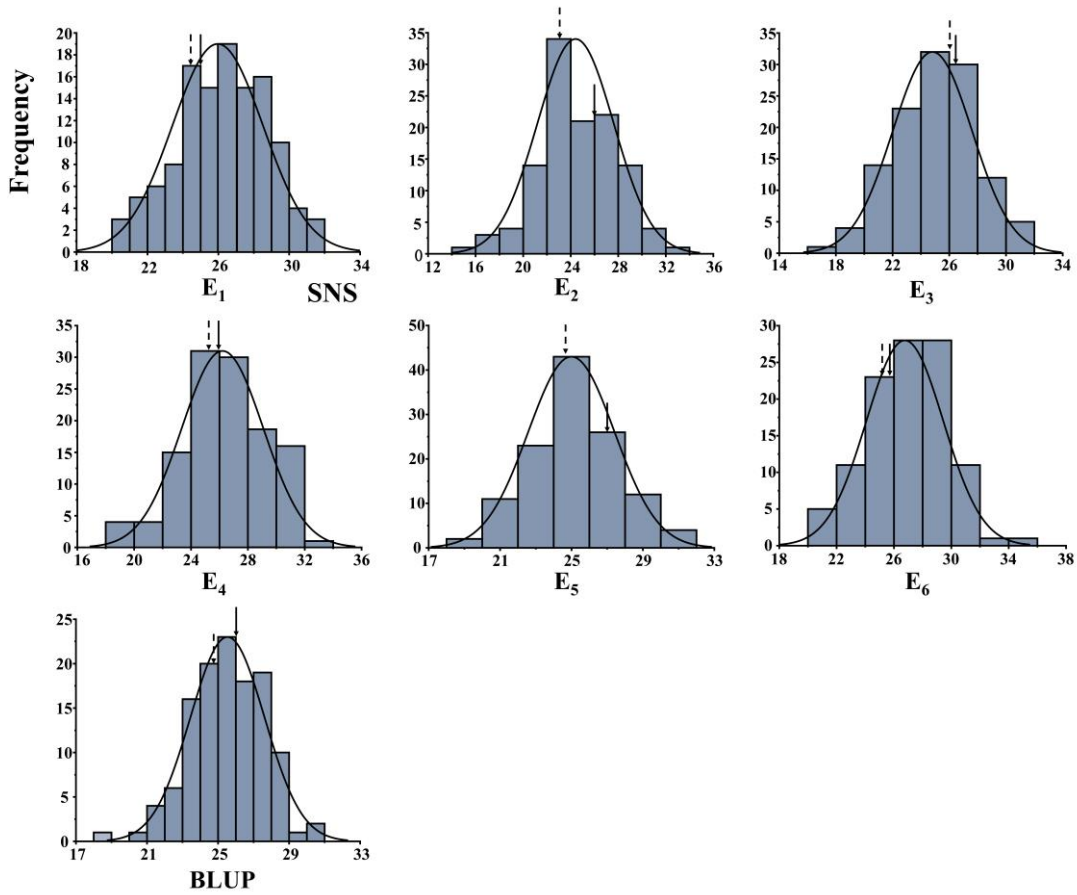

Fig. S2 Frequency distributions of SNS in the AM population from six environments and BLUP. Solid and dotted arrows represented AL and LM001, respectively

Supplementary Tables

Table S1 Environmental information of surveyed agronomic traits

Table S2 The 1150 bin markers used for QTL mapping

Table S3 Comparison of the genetic and physical positions of 6542 mapped markers (including bin markers and co-segregated markers)

Table S4 Quantitative trait loci (QTL) detected in the QTL-by-Environment interaction module

Table S5 Comparison of *QSns.sau-AM-2B.3* and *QSns.sau-AM-3B.2* with previously reported quantitative trait loci (QTL) for spikelet number per spike (SNS) on chromosome 2B and 3B, respectively

Table S6 Predicted genes in the physical interval of the major QTL *QSns.sau-AM-2B.3*

Table S7 Predicted genes in the physical interval of the major QTL *QSns.sau-AM-3B.2*